Particles I

Access the latest eBook →

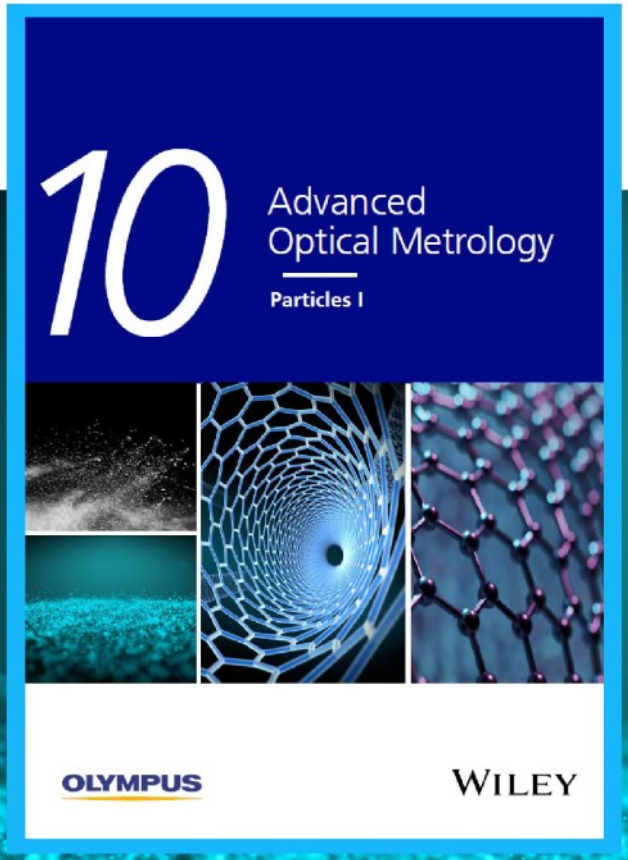

Particles: Unique Properties, Uncountable Applications

Read the latest eBook and better your knowledge with highlights from the recent studies on the design and characterization of micro- and nanoparticles for different application areas.

Access Now

This eBook is sponsored by

OLYMPUS

WILEY

ADVANCED FUNCTIONAL MATERIALS
www.afm-journal.de

Digital Light Processing of Dynamic Bottlebrush Materials

Chungryong Choi, Yoichi Okayama, Parker T. Morris, Lindsay L. Robinson, Matthias Gerst, Joshua C. Speros, Craig J. Hawker, Javier Read de Alaniz,* and Christopher M. Bates**

Bottlebrush elastomers have attracted significant attention as a class of super-soft materials with a storage modulus (G') less than the intrinsic entanglement shear modulus (G_e), but current processing strategies have been limited to molding or extrusion-based 3D printing. Here, the ability to 3D print bottlebrush elastomers via digital light processing (DLP) is demonstrated through the design of novel resin components and building blocks. In particular, mono-telechelic poly(ethylene glycol) (PEG) macromonomers with a 1,2-dithiolane end group derived from α-lipoic acid (LA) undergo fast and efficient copolymerization with PEG diacrylates under light (≤405 nm) in the presence of a photoinitiator to generate crosslinked bottlebrush networks containing dynamic disulfide backbones. This allows objects that are both super-soft and solvent-free to be printed with a commercial DLP printer. The resulting materials undergo dynamic disulfide exchange when exposed to ultraviolet light (365 nm) or elevated temperatures, facilitating reprocessing and postfabrication healing. These results establish a simple design strategy for the preparation of DLP resins based on natural building blocks (α-lipoic acid), leading to materials with unique properties that broaden the utility of light-based 3D printing with user-friendly chemistry.

1. Introduction

3D printing (also known as additive manufacturing) has emerged as an efficient method for fabricating high-fidelity three-dimensional objects with well-defined shapes, sizes, and composition.[1–5] A variety of 3D printing techniques have been developed based on different classes of materials, for example, laser sintering of metals,[6,7] extrusion of thermoplastics,[8] and digital light processing (DLP) of thermosets.[9,10] For polymeric systems, DLP is a powerful 3D printing strategy wherein light is used to photocrosslink a monomer resin, providing spatial and temporal control over local photopolymerization while leveraging advances in optics that have evolved from research throughout the past century in lithography and light-emitting diodes.[11] As a result, DLP offers short processing times, high spatial resolution, and fabrication accuracy with good layer-to-layer adhesion.[9,10]

Given these attractive features of DLP, considerable research has focused on understanding the interplay between photopolymerization kinetics, resin fluid dynamics,[12,13] layer-by-layer versus volumetric exposure,[14–17] and speed–resolution relationships.[12,18,19] These insights have been used in a variety of applications, from customized therapeutics[20–23] to soft-robotics,[24,25] microfluidics,[26–28] and energy harvesting.[29–31] Nevertheless, there remain significant opportunities to develop new resin chemistry for DLP that yields materials with complementary properties to those available today. Here, we focus on two in particular. First, the stiffness (e.g., shear modulus G) of crosslinked polymer networks formed by DLP is typically bounded on the low end by entanglements ($G > G_e$). As has been recognized by Sheiko and co-workers,[4,32,33] many types of biological tissue and muscle have modulus values below this limit. While adding water or organic solvent to form gels further reduces the stiffness of polymer networks (including those 3D printed by extrusion[34–36] and DLP[37,38]), having mobile small molecules present is not always ideal because they can evaporate or leech over time, thus changing the shape of printed parts or creating potential issues with biocompatability. A recent class of materials known as bottlebrush elastomers circumvents these

C. Choi, P. T. Morris, L. L. Robinson, C. J. Hawker, J. Read de Alaniz, C. M. Bates
Department of Chemistry & Biochemistry
University of California
Santa Barbara, CA 93106, USA
E-mail: hawker@mrl.ucsb.edu; javier@chem.ucsb.edu; cbates@ucsb.edu

C. Choi, P. T. Morris, C. J. Hawker, C. M. Bates
Materials Department
University of California
Santa Barbara, CA 93106, USA

The ORCID identification number(s) for the author(s) of this article can be found under https://doi.org/10.1002/adfm.202200883.

DOI: 10.1002/adfm.202200883

Y. Okayama, C. J. Hawker, C. M. Bates
Materials Research Laboratory
University of California
Santa Barbara, CA 93106, USA

M. Gerst
BASF SE
Polymers for Adhesives
67056 Ludwigshafen am Rhein, Germany

J. C. Speros
BASF Corporation California Research Alliance
Berkeley, CA 94720, USA

C. M. Bates
Department of Chemical Engineering
University of California
Santa Barbara, CA 93106, USA

limitations by exploiting polymer architecture to suppress entanglements, which provides access to $G < G_e$ even in bulk networks lacking solvent.[32,39–43] However, to date, bottlebrush elastomers have only been 3D printed by extrusion.[44–46] Second, typical DLP resins produce permanently crosslinked polymer networks (thermosets) that contribute to the plastic waste calamity. Contemporary efforts have addressed this challenge by introducing dynamic bonds, for example, disulfides,[47] esters,[48–50] boronate esters,[10] or Diels–Alder adducts,[51] although these custom resin monomers usually require multiple synthetic steps to access.

Inspired by recent discoveries in sustainable polymeric building blocks,[40] here we demonstrate a new resin platform for 3D printing super-soft ($G < G_e$) and dynamic bottlebrush elastomers by DLP. The simple addition of lipoic-acid-functionalized macromonomers—accessible in one synthetic step from cheap and bio-derived starting materials—to traditional acrylate-based monomer formulations yields resins with fast curing kinetics, generating dynamic and super-soft materials with significantly smaller storage moduli ($G' \approx 100$ kPa) than typical 3D-printed rubbers ($G' \approx 1000$ kPa).[52,53] By virtue of the dynamic disulfide bonds incorporated throughout the polymer network, objects printed from these resins can be reshaped and healed after experiencing damage. These findings expand the types of properties that can be achieved by DLP and add to the contemporary toolbox of resin chemistry for light-based 3D printing.

2. Results and Discussion

Our new DLP resins (**Figure 1**) combine the benefits of two different chemistries: (1) acrylates, which are traditionally used in DLP due to their fast and efficient photopolymerization, and (2) functionalized 1,2-dithiolanes, which can polymerize to form disulfide-containing linear,[54–56] branched,[57] or bottlebrush polymers.[40] Although thermally generated thiyl radicals derived from 1,2-dithiolanes (or similarly elemental sulfur) are known to react with vinyl groups, e.g., in inverse vulcinization,[58–60] to the best of our knowledge no reports have explored photo-*co*polymerization (a key requisite of DLP) using this chemistry.

To create super-soft bottlebrush elastomers by DLP, α-lipoic acid (LA) was introduced to one chain end of linear poly(ethylene glycol) (PEG) with a degree of polymerization $N = 13$ (denoted PEG-LA) through simple esterification (see Figures S1-S3, Supporting Information). Short PEG units were chosen as the macromonomer because they have a low glass transition temperature (T_g), lack crystallinity, and show good solubility with the other resin components. These macromonomers were then copolymerized with a commercially available crosslinker, poly(ethylene glycol)-diacrylate (PEG-DiAc) using phenylbis(2,4,6-trimethylbenzoyl)phosphine oxide (BAPO) as a photoinitiator (Figure 1). Since all components—PEG macromonomer, crosslinker and photoinitiator—mix readily at room temperature, resins with various compositions can be photopolymerized in the absence of solvent, resulting in efficient crosslinking and high gel fractions (see Figures S4 and S5, Supporting Information). This formulation balances the benefits of both monomers; traditional, acrylate-only resins result in permanent covalent bonds after crosslinking, while bottlebrush networks derived from LA-functionalized macromonomers and LA-based crosslinkers are dynamic but thermally unstable, resulting in depolymerization at elevated temperatures (e.g., 180 °C).[40] In addition, this solvent-free approach to building

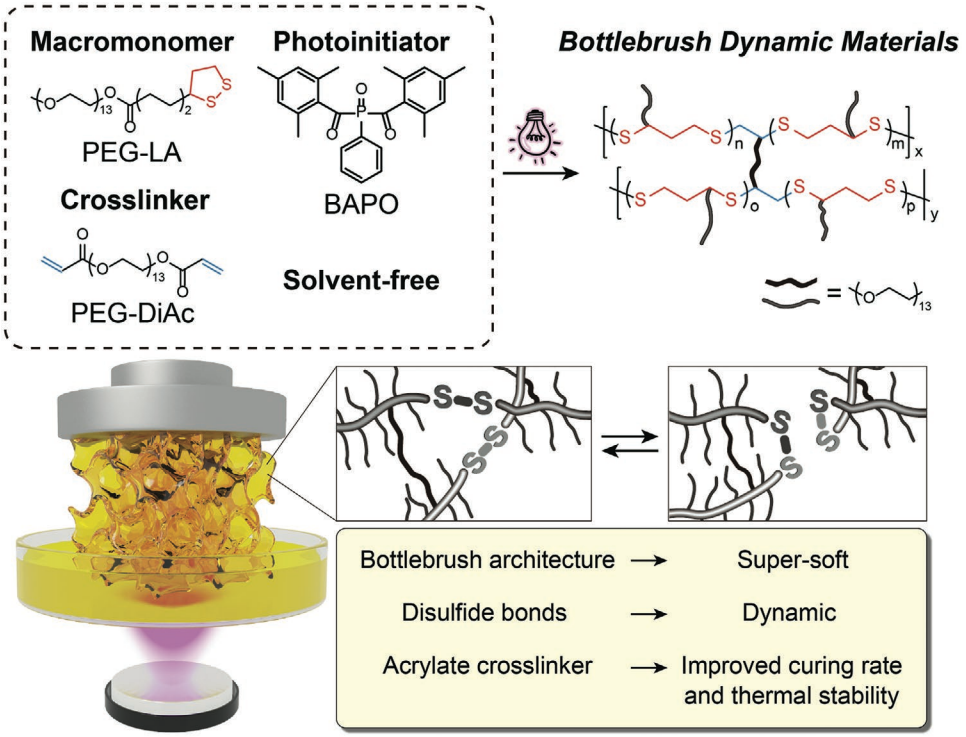

Figure 1. Schematic of digital light processing (DLP) used to 3D print super-soft bottlebrush materials with dynamic disulfide bonds along the backbone.

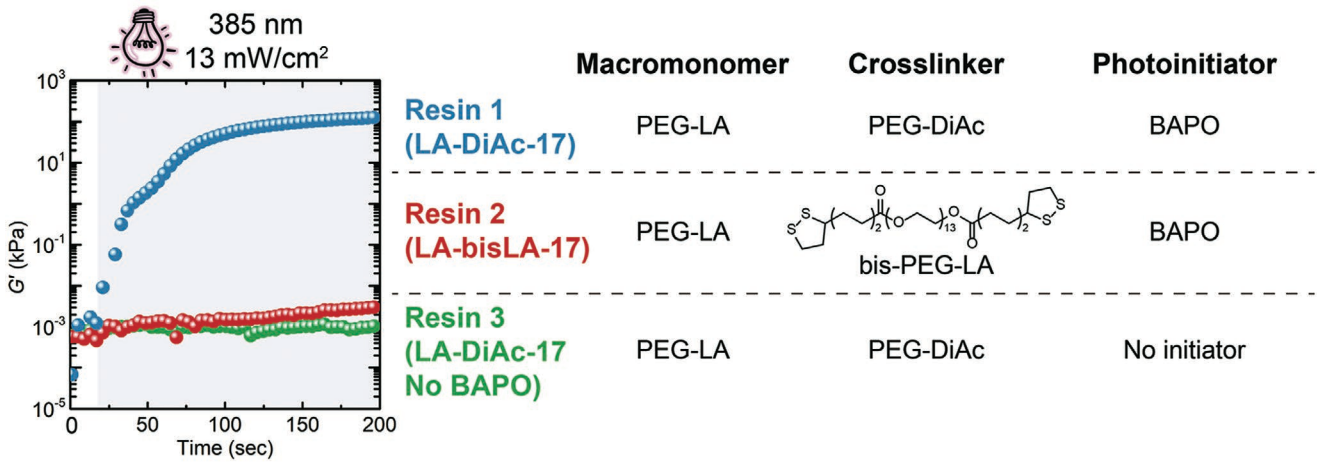

Figure 2. Curing kinetics of three different resins. The copolymerization of a lipoic-acid-derived macromonomer and diacrylate crosslinker (Resin 1: LA-DiAc, blue) results in faster crosslinking, a flatter storage modulus plateau (G'), and a higher gel fraction (93% vs 20%) under irradiation with 385 nm light (13 mW cm^{-2}) compared to Resin 2 (LA-bisLA, red). In the absence of photoinitiator, no reaction occurs (green).

the bottlebrush backbone with light in situ during DLP minimizes resin viscosity effects that would hamper the use of other types of chemistry, e.g., benzophenone crosslinking of presynthesized bottlebrush polymers.[41,46,61]

Importantly, as is evident in **Figure 2**, the formulation containing PEG-LA (83 mol%), PEG-DiAc (17 mol%), and BAPO (Resin 1: "LA-DiAc-17") cures significant faster and to higher conversions under 385 nm light (13 mW cm^{-2}) when compared to a resin system containing only PEG-LA and a lipoic-acid-based crosslinker at the same molar ratio (Resin 2: "LA-bisLA-17," see also Figures S6-S9, Supporting Information). This enhancement in performance with the acrylate–lipoate copolymer resins is crucial for efficient DLP printing. Notably, the LA-DiAc resin also results in a significantly higher gel fraction (93%) than the all-lipoate based systems (20%), LA-bisLA (Figure S10, Supporting Information).

Before 3D printing objects by DLP, we studied the impact of resin composition on material properties for bulk photocrosslinked samples (**Table 1**). Each formulation includes a different ratio of PEG-LA macromonomer to PEG-DiAc crosslinker at constant BAPO photoinitiator loading (2 wt%). As shown in Table 1, samples with at least 17 mol% PEG-DiAc have high gel fractions (≥93%) and low plateau moduli (defined as G' at 0.1 Hz, see Figure S11, Supporting Information), the latter being significantly softer than comparable systems formed from typical acrylate-based resins where the storage shear modulus ≥1 MPa (e.g., methyl acrylate, see Figure S12, Supporting Information).[52,53] As expected, the plateau modulus is lower as the content of macromonomer increases, illustrating the dilution of elastically effective network strands with values reaching 100 kPa at 86 mol% PEG-LA. This minimum modulus could likely be decreased further—to ≈1–10 kPa, values consistent with other bottlebrush elastomers[39,62] and highly solvated, 3D-printed hydrogels[63]—using formulations that yield network strands with bulkier side chains, longer backbones, a higher grafting density, and lower crosslinking density.

Formulations that include PEG-LA generate networks containing disulfide bonds, allowing these materials to perform as dynamic covalent-adaptable networks at elevated temperatures or under UV irradiation (**Figure 3**, Figures S13 and S14, Supporting Information). The characteristic relaxation time τ^* (when $G/G_0 = e^{-1}$) measured by step-strain stress-relaxation experiments depends on the concentration of disulfide groups, i.e., the PEG-LA loading. Measured values of τ^* span more than an order of magnitude (21000–760 s) at 190 °C as PEG-LA increases from 77 to 86 mol%, following Arrhenius behavior as a function of temperature (Figure S13, Supporting Information). We emphasize that these samples containing both PEG-LA and PEG-DiAc are thermally stable (they do not undergo irreversible depolymerization) up to 270 °C, unlike fully lipoate-based networks which contain a higher concentration of disulfide bonds in the bottlebrush network that irreversibly decompose at lower temperatures (Figures S15 and S16,

Table 1. Formulations and properties of LA-DiAc resins studied herein.

Sample name[a)]	PEG-LA [mol%]	PEG-DiAc [mol%]	Plateau modulus [kPa][b)]	Gel fraction [%][c)]	τ^* [s][d)]
LA-DiAc-14	86	14	100	85	760
LA-DiAc-17	83	17	190	93	2700
LA-DiAc-23	77	23	280	95	21 000
DiAc-100	0	100	1200	99	∞

[a)]All samples contain 2 wt% of photoinitiator (BAPO); [b)]Storage modulus at 0.1 Hz; [c)]Measured by dividing the mass of a sample after removing unreacted macromonomers through repeated extraction with THF by the mass immediately after curing; [d)]Determined by a step-strain stress-relaxation experiment at 190 °C.

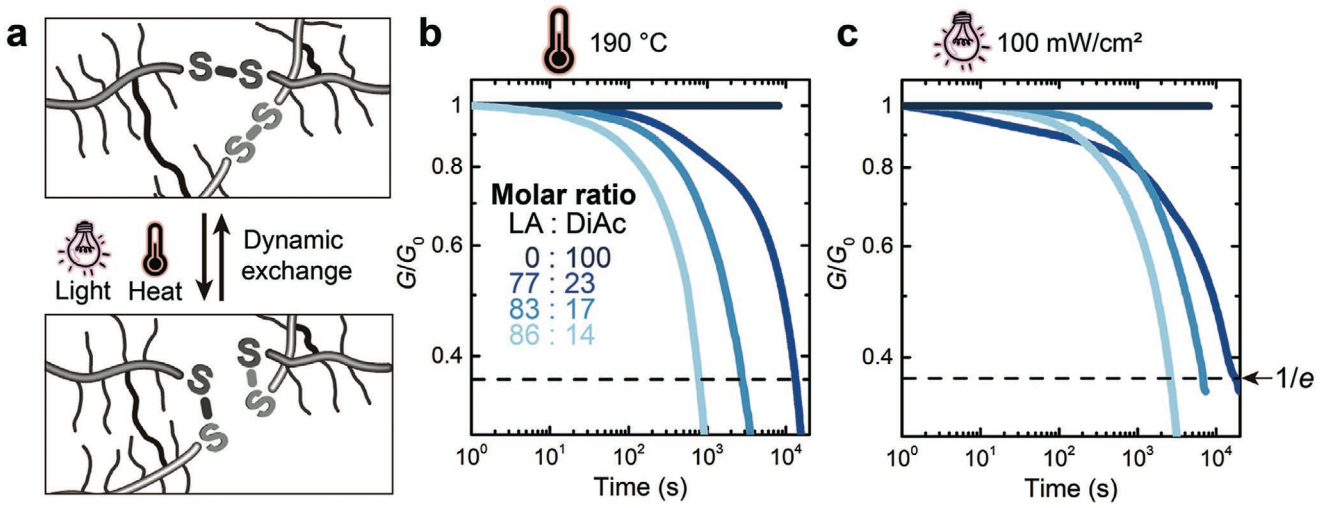

Figure 3. a) Resins containing lipoate-ester macromonomers (PEG-LA) and diacrylate crosslinker (PEG-DiAc) produce dynamic bottlebrush networks that undergo disulfide exchange b) at elevated temperatures (e.g., 190 °C) or c) when exposed to UV/visible light (320–500 nm, 100 mW cm^{-2}). The relaxation dynamics depend on resin composition. G_0: initial modulus, G: stress relaxation modulus.

Supporting Information).[40] Also noteworthy is the stability (non-dynamic nature) of these materials at room temperature (Figure S11, Supporting Information), which facilitates 3D printing under ambient conditions without complications associated with bond exchange and flow (relaxation).[10]

Having identified an optimal resin formulation (LA-DiAc-17, Table 1) with a high gel fraction (93%), super-soft modulus (190 kPa), and dynamic exchange (τ^* = 2700 s), we showcased its efficient 3D photopolymerization by fabricating a variety of objects with a commercially available DLP printer (CELLINK Lumen X+, see Figure S17, Supporting Information). At a wavelength of 385 nm (where BAPO has a maximum absorbance peak, Figure S18, Supporting Information), an optimized layer thickness of 50 µm, exposure time of 1.5 s, and an irradiation intensity of 13 mW cm^{-2} provided the best in-plane resolution (300 µm, see Figure S19, Supporting Information). With these optimized conditions, a double gyroid, icosahedron, octahedron, and gecko were printed with high fidelity (**Figure 4** and Figure S20, Supporting Information). Significantly, the mechanical properties of objects printed in this way are very similar to molded control samples as evaluated by rheometry and tensile testing (Figure S21, Supporting Information). Note that these materials, although super-soft and solvent-free, are fairly brittle; we anticipate further tuning the formulation—for example, through comonomer chemistry, macromonomer length, and grafting density—will provide a route to improve the toughness.

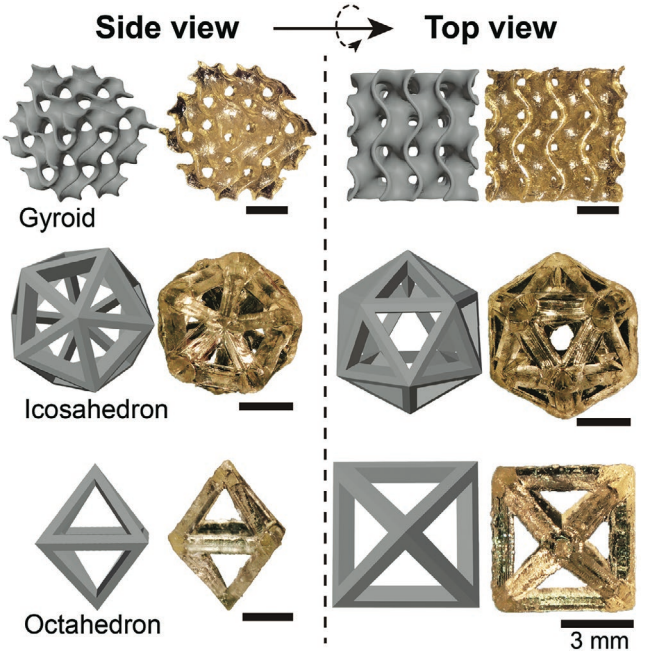

Figure 4. Super-soft and dynamic objects fabricated with a commercial DLP printer from optimized resin LA-DiAc-17; computer models (gray) and photographs (gold). Exposure conditions: wavelength = 385 nm, light intensity = 13 mW cm^{-2}, layer thickness = 50 µm, and exposure time per layer = 1.5 s. All scale bars are 3 mm.

To test the dynamic exchange performance of 3D printed materials, two gecko-inspired objects were subjected to different processing conditions after DLP. One was crushed into a powder and reshaped with heat or light under compression into a rectangular prism and dog bone, respectively (**Figure 5**a, left pathway). Alternatively, the tail of the second gecko was cut and an attempt was made to reconnect it with heat, which was not effective without applying pressure. Instead, we observed that the addition of a strong base such 1,8-diazabicyclo[5.4.0] undec-7-ene (DBU) to the cut surfaces accelerated dynamic exchange without heat or compression, generating a healed interface at room temperature (Figure S23, Supporting Information) that sustained the weight of the gecko body when hung on a wall (Figure 5a, right pathway). This qualitative behavior is consistent with a significant reduction in relaxation time at room temperature (≈200 s, Figure S24, Supporting Information), which we propose is related to the mechanism shown in Figure 5b.[64]

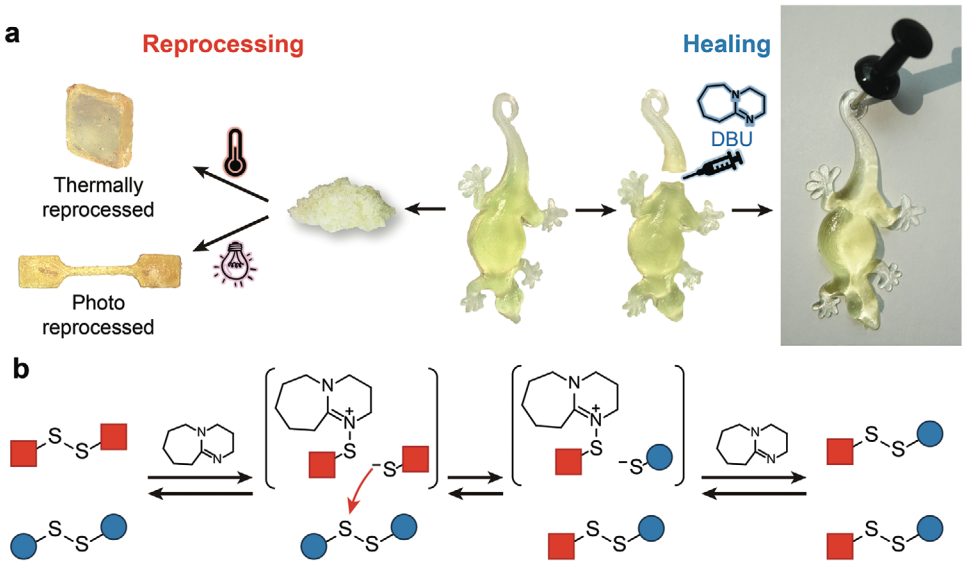

Figure 5. a) Objects printed from the optimized resin LA-DiAc-17 can be reprocessed with heat or light under compression (left) and cut surfaces are healed at room temperature by the addition of 1,8-diazabicyclo[5.4.0]undec-7-ene (DBU, right). b) Proposed mechanism of DBU-mediated self-healing via disulfide exchange.

3. Conclusions

A new class of resins for DLP-based 3D printing was described that generate super-soft, dynamic, and self-healable elastomers under mild conditions using a commercially available printer and convenient exposure conditions. These advances are enabled by the fast and efficient copolymerization of lipoate-ester-based macromonomers with diacrylate crosslinkers, leading to bottlebrush networks containing disulfide units. Such design insights expand the range of properties that can be achieved with DLP and create unique opportunities to tailor the performance of advanced materials fabricated by light.

4. Experimental Section

Detailed experimental methods are described in the Supporting Information. PEG-LA and bis-PEG-LA were synthesized from poly(ethylene glycol methyl ether) (PEG-OH) and dihydroxy PEG (HO-PEG-OH) via EDC/DMAP esterification. PEG-diacrylate (PEG-DiAc) was used after removing inhibitor. BAPO was used as received.

In situ UV–rheometry experiments were conducted using a UV-curing accessory on an ARES-G2 equipped with a 385 nm light emitting diode at 1% strain and a frequency of 1 Hz. Modulus changes during stress relaxation were measured at elevated temperatures or under UV–vis light at a fixed strain of 1.5%. All 3D objects were printed with a Lumen X+ DLP printer operating at 385 nm. The thickness of each layer was set at 50 µm with the irradiation intensity and time for printing each layer being 13 mW cm^{-2} and 1.5 s, respectively. UV intensities reported for UV–rheometry and 3D printing were measured using a photometer (Silverline UV Radiometer). For thermal and photo reprocessing, a crushed powder was placed into a stainless-steel mold, sandwiched between glass slides, and pressed with binder clips. For thermal reprocessing, the sample was placed in an oven at 200 °C for 48 h. For photo reprocessing, the sample was held under UV light (365 nm) with an intensity of 60 mW cm^{-2} for 48 h. To heal the gecko's snipped tail, DBU was coated on the cut surface using capillary action with the sample subsequently kept under ambient conditions for 24 h.

Supporting Information

Supporting Information is available from the Wiley Online Library or from the author.

Acknowledgements

The authors thank the BASF California Research Alliance (CARA) for funding (C.C.). The research reported here was supported by the National Science Foundation under Award No. CMMI-2053760 (C.M.B.) and partially supported by the BioPACIFIC Materials Innovation Platform of the National Science Foundation under Award No. DMR-1933487. C.J.H. thanks the U.S. Army Research Office under Cooperative Agreement W911NF-19-2-0026 and under Contract Number W911NF-19-D-0001 for the Institute for Collaborative Biotechnologies. Y.O. thanks Nippon Shokubai Ltd. for funding. L.L.R. was supported by a National Science Foundation Graduate Research Fellowship under Grant No. 1650114. The research reported here made use of shared facilities of the UC Santa Barbara Materials Research Science and Engineering Center (MRSEC, NSF-DMR 1720256), a member of the Materials Research Facilities Network (www.mrfn.org).

Conflict of Interest

The authors declare no conflict of interest.

Data Availability Statement

The data that support the findings of this study are available in the supplementary material of this article.

Keywords

bottlebrush elsatomers, super-soft elastomers, 3D printing, digital light processing

Received: January 21, 2022
Revised: February 2, 2022
Published online:

[1] R. L. Truby, J. A. Lewis, *Nature* **2016**, *540*, 371.
[2] S. C. Ligon, R. Liska, J. Stampfl, M. Gurr, R. Mulhaupt, *Chem. Rev.* **2017**, *117*, 10212.
[3] J. Herzberger, J. M. Sirrine, C. B. Williams, T. E. Long, *Prog. Polym. Sci.* **2019**, *97*, 101144.
[4] L. Y. Zhou, J. Fu, Y. He, *Adv. Funct. Mater.* **2020**, *30*, 2000187.
[5] L. J. Tan, W. Zhu, K. Zhou, *Adv. Funct. Mater.* **2020**, *30*, 2003062.
[6] M. Agarwala, D. Bourell, J. Beaman, H. Marcus, J. Barlow, *Rapid Prototyping J.* **1995**, *1*, 26.
[7] A. Simchi, *Mater. Sci. Eng., A* **2006**, *428*, 148.
[8] J. A. Lewis, G. M. Gratson, *Mater. Today* **2004**, *7*, 32.
[9] A. Bagheri, J. Jin, *ACS Appl. Polym. Mater.* **2019**, *1*, 593.
[10] L. L. Robinson, J. L. Self, A. D. Fusi, M. W. Bates, J. Read de Alaniz, C. J. Hawker, C. M. Bates, C. S. Sample, *ACS Macro Lett.* **2021**, *10*, 857.
[11] C. Sun, N. Fang, D. M. Wu, X. Zhang, *Sens. Actuators, A* **2005**, *121*, 113.
[12] J. R. Tumbleston, D. Shirvanyants, N. Ermoshkin, R. Janusziewicz, A. R. Johnson, D. Kelly, K. Chen, R. Pinschmidt, J. P. Rolland, A. Ermoshkin, E. T. Samulski, J. M. DeSimone, *Science* **2015**, *347*, 1349.
[13] R. Janusziewicz, J. R. Tumbleston, A. L. Quintanilla, S. J. Mecham, J. M. DeSimone, *Proc. Natl. Acad. Sci. U. S. A.* **2016**, *113*, 11703.
[14] B. E. Kelly, I. Bhattacharya, H. Heidari, M. Shusteff, C. M. Spadaccini, H. K. Taylor, *Science* **2019**, *363*, 1075.
[15] M. Shusteff, A. E. M. Browar, B. E. Kelly, J. Henriksson, T. H. Weisgraber, R. M. Panas, N. X. Fang, C. M. Spadaccini, *Sci. Adv.* **2017**, *3*, 5496.
[16] D. A. Walker, J. L. Hedrick, C. A. Mirkin, *Science* **2019**, *366*, 360.
[17] D. Loterie, P. Delrot, C. Moser, *Nat. Commun.* **2020**, *11*, 852.
[18] D. Ahn, L. M. Stevens, K. Zhou, Z. A. Page, *ACS Cent. Sci.* **2020**, *6*, 1555.
[19] X. Zhao, Y. Zhao, M. D. Li, Z. Li, H. Peng, T. Xie, X. Xie, *Nat. Commun.* **2021**, *12*, 2873.
[20] C. Caudill, J. L. Perry, K. Iliadis, A. T. Tessema, B. J. Lee, B. S. Mecham, S. Tian, J. M. DeSimone, *Proc. Natl. Acad. Sci. U. S. A.* **2021**, *118*, e2102595118.
[21] M. E. Prendergast, J. A. Burdick, *Adv. Mater.* **2020**, *32*, 1902516.
[22] H. J. Oh, M. S. Aboian, M. Y. J. Yi, J. A. Maslyn, W. S. Loo, X. Jiang, D. Y. Parkinson, M. W. Wilson, T. Moore, C. R. Yee, G. R. Robbins, F. M. Barth, J. M. DeSimone, S. W. Hetts, N. P. Balsara, *ACS Cent. Sci.* **2019**, *5*, 419.
[23] J. Norman, R. D. Madurawe, C. M. Moore, M. A. Khan, A. Khairuzzaman, *Adv. Drug. Delivery Rev.* **2017**, *108*, 39.
[24] T. J. Wallin, J. Pikul, R. F. Shepherd, *Nat. Rev. Mater.* **2018**, *3*, 84.
[25] N. W. Bartlett, M. T. Tolley, J. T. B. Overvelde, J. C. Weaver, B. Mosadegh, K. Bertoldi, G. M. Whitesides, R. J. Wood, *Science* **2015**, *349*, 161.
[26] N. Bhattacharjee, A. Urrios, S. Kang, A. Folch, *Lab Chip* **2016**, *16*, 1720.
[27] S. Waheed, J. M. Cabot, N. P. Macdonald, T. Lewis, R. M. Guijt, B. Paull, M. C. Breadmore, *Lab Chip* **2016**, *16*, 1993.
[28] G. Weisgrab, A. Ovsianikov, P. F. Costa, *Adv. Mater. Technol.* **2019**, *4*, 1900275.
[29] K. Fu, Y. Wang, C. Yan, Y. Yao, Y. Chen, J. Dai, S. Lacey, Y. Wang, J. Wan, T. Li, Z. Wang, Y. Xu, L. Hu, *Adv. Mater.* **2016**, *28*, 2587.
[30] A. Ambrosi, M. Pumera, *Chem. Soc. Rev.* **2016**, *45*, 2740.
[31] K. Fu, Y. Yao, J. Dai, L. Hu, *Adv. Mater.* **2017**, *29*, 1603486.
[32] M. Vatankhah-Varnosfaderani, W. F. M. Daniel, M. H. Everhart, A. A. Pandya, H. Y. Liang, K. Matyjaszewski, A. V. Dobrynin, S. S. Sheiko, *Nature* **2017**, *549*, 497.
[33] A. Vedadghavami, F. Minooei, M. H. Mohammadi, S. Khetani, A. R. Kolahchi, S. Mashayekhan, A. Sanati-Nezhad, *Acta Biomater.* **2017**, *62*, 42.
[34] B. Narupai, P. T. Smith, A. Nelson, *Adv. Funct. Mater.* **2021**, *31*, 2011012.
[35] A. Basu, A. Saha, C. Goodman, R. T. Shafranek, A. Nelson, *ACS Appl. Mater. Interfaces* **2017**, *9*, 40898.
[36] P. T. Smith, A. Basu, A. Saha, A. Nelson, *Polymer* **2018**, *152*, 42.
[37] E. Sanchez-Rexach, P. T. Smith, A. Gomez-Lopez, M. Fernandez, A. L. Cortajarena, H. Sardon, A. Nelson, *ACS Appl. Mater. Interfaces* **2021**, *13*, 19193.
[38] Z. Y. Ji, C. Y. Yan, B. Yu, X. Q. Zhang, M. R. Cai, X. Jia, X. L. Wang, F. Zhou, *Adv. Mater. Technol.* **2019**, *4*, 1800713.
[39] W. F. M. Daniel, J. Burdynska, M. Vatankhah-Varnoosfaderani, K. Matyjaszewski, J. Paturej, M. Rubinstein, A. V. Dobrynin, S. S. Sheiko, *Nat. Mater.* **2016**, *15*, 183.
[40] C. Choi, J. L. Self, Y. Okayama, A. E. Levi, M. Gerst, J. C. Speros, C. J. Hawker, J. Read de Alaniz, C. M. Bates, *J. Am. Chem. Soc.* **2021**, *143*, 9866.
[41] S. Mukherjee, R. X. Xie, V. G. Reynolds, T. Uchiyama, A. E. Levi, E. Valois, H. B. Wang, M. L. Chabinyc, C. M. Bates, *Macromolecules* **2020**, *53*, 1090.
[42] M. Abbasi, L. Faust, M. Wilhelm, *Adv. Mater.* **2019**, *31*, 1806484.
[43] L. H. Cai, T. E. Kodger, R. E. Guerra, A. F. Pegoraro, M. Rubinstein, D. A. Weitz, *Adv. Mater.* **2015**, *27*, 5132.
[44] E. Dashtimoghadam, F. Fahimipour, A. N. Keith, F. Vashahi, P. Popryadukhin, M. Vatankhah-Varnosfaderani, S. S. Sheiko, *Nat. Commun.* **2021**, *12*, 3961.
[45] S. F. Nian, J. C. Zhu, H. Z. Zhang, Z. H. Gong, G. Freychet, M. Zhernenkov, B. X. Xu, L. H. Cai, *Chem. Mater.* **2021**, *33*, 2436.
[46] R. X. Xie, S. Mukherjee, A. E. Levi, V. G. Reynolds, H. B. Wang, M. L. Chabinyc, C. M. Bates, *Sci. Adv.* **2020**, *6*, 6900.
[47] X. P. Li, R. Yu, Y. Y. He, Y. Zhang, X. Yang, X. J. Zhao, W. Huang, *ACS Macro Lett.* **2019**, *8*, 1511.
[48] B. Zhang, K. Kowsari, A. Serjouei, M. L. Dunn, Q. Ge, *Nat. Commun.* **2018**, *9*, 1831.
[49] E. Rossegger, R. Höller, D. Reisinger, J. Strasser, M. Fleisch, T. Griesser, S. Schlögl, *Polym. Chem.* **2021**, *12*, 639.
[50] E. Rossegger, K. Moazzen, M. Fleisch, S. Schlögl, *Polym. Chem.* **2021**, *12*, 3077.
[51] X. P. Li, R. Yu, Y. Y. He, Y. Zhang, X. Yang, X. J. Zhao, W. Huang, *Polymer* **2020**, *200*, 122532.
[52] J. Borrello, P. Nasser, J. Iatridis, K. D. Costa, *Addit. Manuf.* **2018**, *23*, 374.
[53] M. Lebedevaite, V. Talacka, J. Ostrauskaite, *J. Appl. Polym. Sci.* **2020**, *138*, 50233.
[54] T. Suzuki, Y. Nambu, T. Endo, *Macromolecules* **1990**, *23*, 1579.
[55] A. Kisanuki, Y. Kimpara, Y. Oikado, N. Kado, M. Matsumoto, K. Endo, *J. Polym. Sci., Part A: Polym. Chem.* **2010**, *48*, 5247.
[56] C. T. Richard, J. R. Lester, *J. Am. Chem. Soc.* **1956**, *78*, 6148.
[57] H. Tang, N. V. Tsarevsky, *Polym. Chem.* **2015**, *6*, 6936.
[58] W. J. Chung, J. J. Griebel, E. T. Kim, H. Yoon, A. G. Simmonds, H. J. Ji, P. T. Dirlam, R. S. Glass, J. J. Wie, N. A. Nguyen, B. W. Guralnick, J. Park, A. Somogyi, P. Theato, M. E. Mackay, Y. E. Sung, K. Char, J. Pyun, *Nat. Chem.* **2013**, *5*, 518.
[59] X. Wu, J. A. Smith, S. Petcher, B. Zhang, D. J. Parker, J. M. Griffin, T. Hasell, *Nat. Commun.* **2019**, *10*, 647.
[60] Q. Zhang, C. Y. Shi, D. H. Qu, Y. T. Long, B. Feringa, H. Tian, *Sci. Adv.* **2018**, *4*, 8192.
[61] V. G. Reynolds, S. Mukherjee, R. X. Xie, A. E. Levi, A. Atassi, T. Uchiyama, H. B. Wang, M. L. Chabinyc, C. M. Bates, *Mater. Horiz.* **2020**, *7*, 181.
[62] M. Vatankhah-Varnoosfaderani, W. F. M. Daniel, A. P. Zhushma, Q. X. Li, B. J. Morgan, K. Matyjaszewski, D. P. Armstrong, R. J. Spontak, A. V. Dobrynin, S. S. Sheiko, *Adv. Mater.* **2017**, *29*, 1604209.
[63] J. Odent, T. J. Wallin, W. Y. Pan, K. Kruemplestaedter, R. F. Shepherd, E. P. Giannelis, *Adv. Funct. Mater.* **2017**, *27*, 1701807.
[64] Z. Q. Lei, H. P. Xiang, Y. J. Yuan, M. Z. Rong, M. Q. Zhang, *Chem. Mater.* **2014**, *26*, 2038.